Semi-automatic segmentation analysis of adipose tissue in thigh and lower leg to assess the fat infiltration in Type 2 Diabetes Mellitus

Sunil K. Valaparla[1,2], Qi Peng[3], Feng Gao[1], Timothy Q. Duong[1], and Geoffrey D. Clarke[1,2]

[1]Research Imaging Institute, University of Texas Health Science Center at San Antonio, San Antonio, Texas, United States, [2]Radiology, University of Texas Health Science Center at San Antonio, San Antonio, Texas, United States, [3]Department of Radiology, Albert Einstein College of Medicine, Bronx, NY, United States

Target Audience: MR researchers interested in distribution of skeletal muscle adipose tissue in Type 2 Diabetes Mellitus (T2DM)

Introduction: T2DM and insulin resistance have been associated with increase in amount and distribution of visceral adipose tissue and intermuscular adipose tissue (IMAT) (1). IMAT is composed of adipocytes located between the muscle fibers and beneath the muscle fascia and represents a useful index to glucose disposal, muscle function and monitoring the effect of nutrition and exercise in metabolic abnormalities (1-2). Accurate determination of spatially heterogeneous IMAT in localized regions would ideally require high spatial-resolution and efficient fat water contrast enhanced MR imaging methods measuring the proton density-weighted fat fraction corrected for RF coil sensitivity and partial-volume effects. Several image analysis algorithms were developed for abdominal fat distribution assessment and are widely validated, but development of dedicated tools for assessment of fat distribution in the extremities is still in an early stage, and image analysis was usually performed manually requiring longer processing time and affected by observer-induced variability (4). The purpose of this study was to evaluate a semi-automated fuzzy clustering (FCT) segmentation algorithm (3) in investigating the differences in the quantity and regional distribution of IMAT and SAT in the high-resolution T_1-weighted thigh and lower leg images between patients with T2DM and healthy controls.

Methods: Fourteen subjects (7 controls, age: 30.2 ± 4.8 yrs, BMI: 25.5 ± 4 kg/m^2; and 7 T2DM subjects, age: 55.1 ± 6.4 yrs, BMI: 31.3 ± 3.2 kg/m^2) participated in this study. MR examinations were performed on a 3T MRI (Magnetom Tim Trio; Siemens Healthcare, Erlangen, Germany) after overnight fasting. High resolution T_1-weighted images of right thigh and lower leg were recorded by a fast-spin-echo sequence with the following measurement parameters: TR / TE = 700 / 25 ms, echo train length = 4, slices = 12, slice thickness = 5 mm, in-plane resolution = 0.7 x 0.5 mm^2, α =120°, GRAPPA = 2, 2D acquisition time = 90 s, BW = 250 Hz/Px. Subjects were lying in supine position with the mid-section of the thigh and lower leg centered in the 4-channel wrap-around flexible phase array coil in two separate acquisitions.

Data Analysis: All images are corrected for spatial intensity variations (bias field or RF inhomogeneity) using FSL FAST v4.0 (5). Skeletal muscle adipose tissue analysis was performed using QFAT 2.2 (IDL, Research Systems, Boulder, CO). First, minimal entropy of the image grayscale histogram was obtained by iteratively applying 2D polynomial field correction. Second, fat pixels were segmented from nonfat pixels by a fully automated FCT method to generate a fat-only image. Two threshold values were set to distinguish muscle tissue (NAT), and AT. The threshold value between NAT and AT was changed manually after visual inspection of the original image and the segmented fat image. Third SAT, IMAT and fatty bone-marrow voxels were identified based on contours separating the exterior (red) and internal (green) boundary of SAT and bone (yellow, blue), generated with an automated chain-code algorithm for boundary detection. The automated contours were then manually corrected to include accurate localization of SAT and IMAT by excluding bone and lean muscle. IMAT was determined by subtracting the area of SAT from total AT. Finally, SAT and IMAT mean slice volume (cm^3) of thigh and lower leg were calculated by multiplying the number of relevant pixels by the pixel dimensions and slice thickness for 12 slices. Two-tailed Student t-tests were used to compare SAT and IMAT from thigh and lower leg between the two subject groups. All statistical analyses were performed with R 3.0.2 statistical software. P < 0.05 was considered statistically significant.
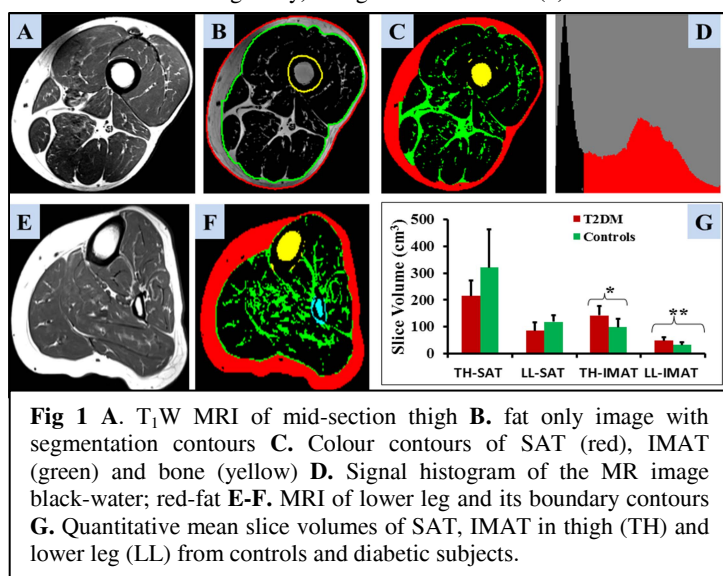
Fig 1 A. T_1W MRI of mid-section thigh **B.** fat only image with segmentation contours **C.** Colour contours of SAT (red), IMAT (green) and bone (yellow) **D.** Signal histogram of the MR image black-water; red-fat **E-F.** MRI of lower leg and its boundary contours **G.** Quantitative mean slice volumes of SAT, IMAT in thigh (TH) and lower leg (LL) from controls and diabetic subjects.

Results and Discussion: Two-tailed Student t-test with equal variances showed no statistical significance between T2DM and Controls for thigh TH-SAT (-56.68cm^3 less, p = 0.517); TH-IMAT (42.81cm^3 less, p*= 0.062) and for lower leg LL-SAT (-20.72cm^3 less, p = 0.310) but was significant for LL-IMAT (15.99cm^3 less, p** = 0.0369). Controls SAT mean slice volume had the highest CV = 54.71% and T2DM IMAT volumes produced lowest CV = 25.37% for a subject sample size n=7 per group. Between the two compartments of thigh and lower leg, SAT was larger in size than IMAT in both groups. T_1W MRI at 3T with a phase-array coil had strong B_0 and B_1 inhomogeneities leading to image intensity non-uniformities and was effectively corrected in this study. Some limitations in this study include a small number of subjects per group and standard spin echo T_1W MRI commonly used in clinical practice was adopted in the validation. However, IDEAL (2) and water-suppressed sequences optimized for fat assessment could increase the contrast between fat and nonfat tissues and could improve the effectiveness of image segmentation algorithm. Segmentation analysis did not characterize difference in the distribution of subfascial fat as it was included in the contour for IMAT computation. Future studies will focus on examining the mechanisms in skeletal muscle adipose tissue distribution linking to age, gender and race matched for BMI.

Conclusion: Semi-automated fuzzy c-mean segmentation algorithm with low computational complexity and processing time enables effective characterization of regional distribution of muscular fat in MR images and can be used to assess IMAT for large-scale clinical imaging studies. The results of the present study are consistent with a previous study (2) showing that a lower volume of subcutaneous fat compared to the controls characterizes T2DM. The results of the present study do not show any statistically significant differences in the SAT and IMAT volume between the groups of T2DM and controls.

References: [1] Michael Boettcher et al. JMRI 2009; 29:1340–1345, [2] Dimitrios C. Karampinos et al. JMRI 2012; 35:899–907 [3] Anqi Zhou et al. JMRI 2011; 34:852–860, [4] Vincenzo Positano et al. JMRI 2009; 29:677–684. [5] Zhang Y.et al. IEEE Trans Med Imag, 2001 20(1):45-57